Resolution enhancement with deconvolution after migration

John C. Bancroft, Thais Guirigay, Naser Yousefzadeh, and Helen Isaac

ABSTRACT

Deconvolution is a process that is normally applied to seismic data before migration to enhance the resolution. We propose that deconvolution should also be applied to the data after a poststack or a prestack migration. We address the objections to this process, then present arguments for its use. The deconvolution process should be applied as a multidimensional process to the complete data. However, a typical trace process is usually sufficient to provide a significant enhancement in the resolution after migration. Two data examples are provided that show significant improvement in the resolution of the data by use of a simple spiking deconvolution that was applied to each trace after migration.

INTRODUCTION

Deconvolution

We propose that deconvolution should be applied after migration and refer to this process as DaM. Ideally the deconvolution process should have dimensions equal to that of the migrated data. However, a 1D deconvolution of a vertical trace, (trace deconvolution) is usually sufficient to enhance the resolution of the migrated data. We have been applying this process for many years and are aware that "others" have also been applying DaM, but refer to it as spectral whitening, or some related form that is often associated with high resolution acquisition. We have also encountered significant opposition to applying DaM, and our intent is to discuss some of the objections and present reasons for it use.

We commence by reviewing the resolution of wavelets before and after migration, review the objections to DaM, then present the reasons for applying DaM. Two examples of real data are shown that illustrate the benefit of the process when a simple spiking deconvolution is used.

Much of the discussion is illustrated using a Kirchhoff type algorithm that is conveniently described with Linear Algebra (or matrix theory); however, the principles do apply to all methods of migration. We also present a simplified description of modelling seismic data using reflectivity and diffraction matrices, then estimate the reflectivity using the seismic and diffraction matrix using Least Squares Migration (LSM). We then show that conventional migration is a simplification of LSM. These concepts are well known in the seismic industry, and have been included here to help identify the deficiencies of conventional migrations (Claerbout 1992).

LSM is an optimum form of seismic inversion as it recovers the highest resolution of the reflectivity when using a linear process. As a migration, it does require a reasonably accurate velocity model, and can be used to refine and update that velocity model (Yousefzadeh et al. 2013). It should not be confused with Full Waveform Inversion

(FWI) that uses migration as part of an iterative process to estimate “rock properties”. The higher resolution of LSM may aid in refining FWI to converge at a faster rate.

A typical one dimensional deconvolution process, used in seismic processing, defines an operator from a time window which is then applied to each trace: we refer to this process as a trace deconvolution. An alternate deconvolution may be applied to a section of data similar to image sharpening in photo processing. We refer to this process as a multidimensional deconvolution.

A great deal of seismic data can be migrated with a time migration where deconvolution after migration is a reasonably straight forward process as the traces are in time. Deconvolution after a depth migration is not straightforward. In a typical medium where the velocities increase with depth, the compression of a wavelet in a depth trace is more extreme that in a corresponding wavelet in a time trace. In a deeper part of the section, the stretching of the wavelet in a depth trace is more severe than in a corresponding time trace. This larger range in the size of the wavelet increases the non-stationarity of a depth trace, making simple deconvolution difficult. However, a simple conversion from vertical depth to vertical time may allow conventional time deconvolution to be applied.

An earlier and simplified version of this paper was presented in the CSEG Recorder magazine (Bancroft 2012).

A summary of objections to deconvolving data after migration

Deconvolving data after migration (DaM) has met with considerable objection when requested by the authors. Some of these objections are;

1. Deconvolution before migration maintains the resolution of horizontal and dipping events and DaM is not necessary,
2. Deconvolution may alias the frequencies of steeply dipping migrated events,
3. Deconvolution will increase noise,
4. Deconvolution will produce artifacts, and
5. Kirchhoff migration already uses whitening operators and DaM is not necessary.

REVIEW OF SEISMIC BASICS

The movement of the wavelet

Consider a zero-offset geophysical model where a wavelet is stationary and assumed to be defined by the source. The zero-offset raypaths are normal to the reflectors. The reflection energy is plotted below the source/receiver location to form a seismic section, even when coming from a dipping reflector, as illustrated in Figure 1a. The reflection events on the section (b) will contain the same wavelet, independent of the dip, and will have the same frequency content. After migration, these wavelets are “rotated” back to the geological location. Deconvolution of the data in (b) will maintain the same resolution of the wavelet in both events after migration.

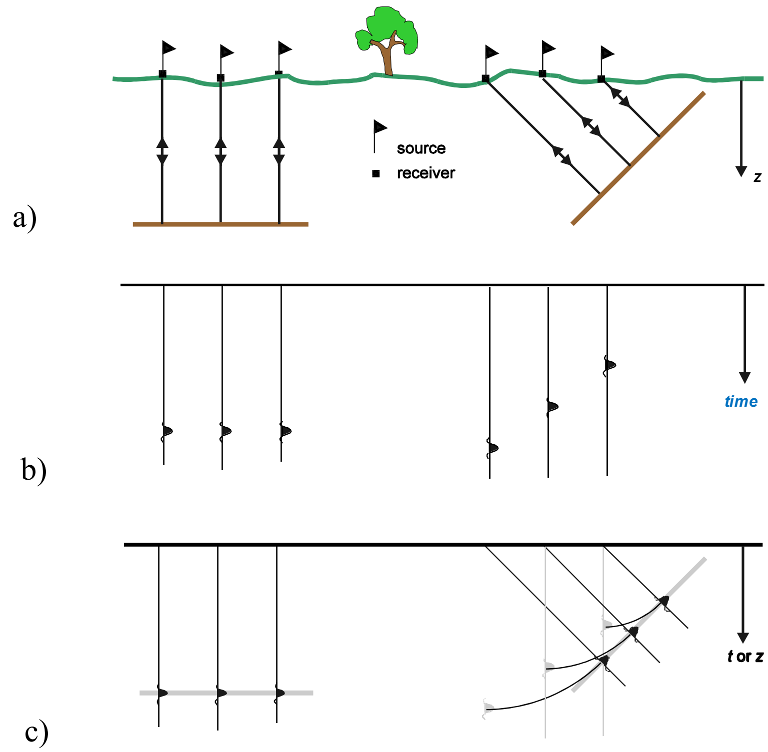

FIG. 1 Cartoon of a) raypaths, b) recorded traveltimes and wavelets, and c) wavelets migrated back to the reflector.

The resolution of the two reflections is compared before and after a poststack migration in Figure 2. The seismic data before migration in Figure 2a has a horizontal reflection and a dipping reflection with dip α. After migration, the horizontal event remains the same, but the dipping reflector in Figure 2b has a dip β as related by the migrator's equation $\tan\alpha = \sin\beta$. The black circles in Figure 2a identify the distances between the wavelet minima when measured vertically along the trace, and are used to represent the vertical resolution. The black dashed circle has the same diameter and represents the same wavelet on the vertical traces of the dipping event. It is compared to the smaller diameter blue circle that is measured normal to the dipping event. The resolution of the dipping event, when measured normal to the dip, is higher than the horizontal event.

After migration, the same black circles are shown in Figure 2b, illustrating that the resolution of the horizontal event after migration remains the same. The resolution of the dipping reflector, when measured normal to the reflector, is now the same as the horizontal reflector. The red wavelet is identical to the vertical wavelets in Figure 2a. The green circle represents the new lower wavelength of the dipping event when measured vertical along a trace. The lower frequency in a vertical trace is a natural part of the migration process that prevents aliasing of the dipping event.

It is curious to note that the actual resolution of the dipping event is greater than the horizontal event before migration, but the same after migration.

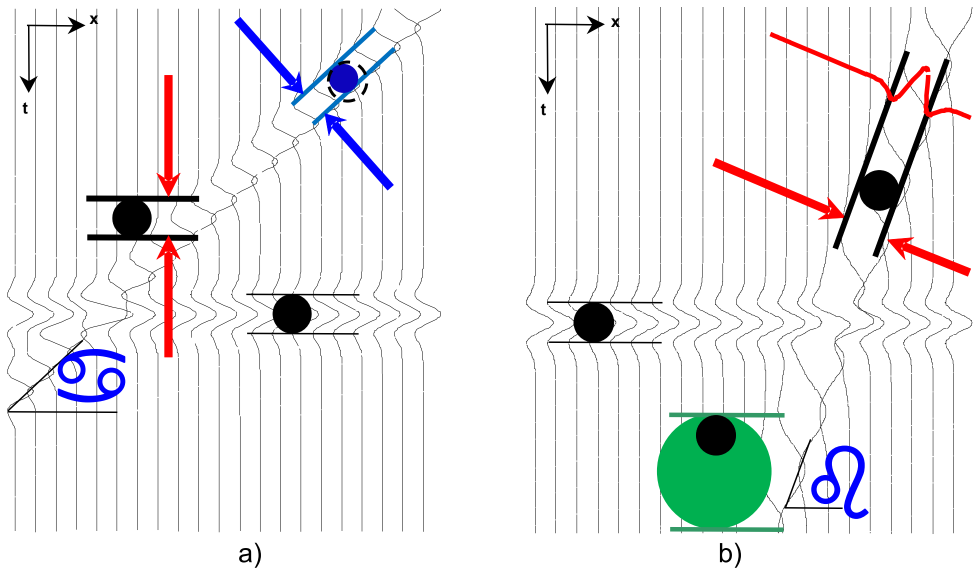

FIG. 2 Seismic events a) before migration and b) after migration.

The FK view

An alternate view of the migration process is illustrated in Figure 3 that shows the location of energy before and after migration in the frequency-wavenumber (FK) domain in a constant velocity medium. The origin is at the bottom center. The trace interval for the seismic data was chosen to match the Nyquist wavenumber to the equivalent maximum frequency of the data. On the left in (a) we see the seismic data contained in a blue triangle that is bound by the maximum frequency and the maximum seismic dip of forty five degrees. After migration, the energy is confined within the blue semicircle in (b). Migration moves energy at dip α in (a) vertically down to dip β in (b). Seismic energy at forty five degrees moves vertically down to a maximum dip of ninety degrees, as illustrated by the black dots.

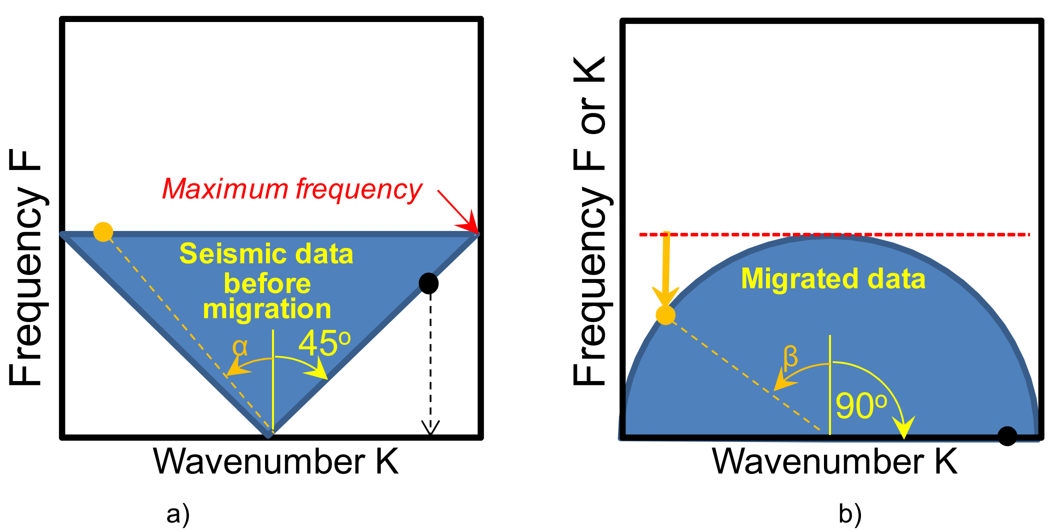

FIG. 3 FK displays of seismic data a) before migration, and b) after migration.

Seismic reflection and diffraction energy, before migration, is confined to dips less than forty five degrees. Any energy with dips above forty five degrees is considered to be noise, which should be over-written by the migration process and eliminated. We used the word "should" because some migrations intentionally leave some of this noise for appearance purposes, or are unable to remove it.

The frequency of the dipping event when measured along the dip in Figure 3a is greater than the frequency of a vertical event with zero dip, indicating it has a higher resolution as indicated in Figure 2a. After migration, all dips have the same resolution (radius) when measured along the dip in Figure 3b, but will have a lower frequency wavelet when measured vertically along a trace as indicated by the orange arrow in the FK domain.

Seismic diffractions

A typical Kirchhoff migration sums the energy in a diffraction. The diffraction can have many forms such as:

- a single valued function (one value for each spatial location), computed analytically for each use,
- a single valued function estimated from Eikonal wavefront mapping, and stored as vectors of traveltime and amplitude,
- a single or multivalued function computed from raytracing that stores the arrival times and amplitudes in vectors, or
- computed using wavefield propagation through a complex medium, and stored in 2D or 3D arrays.

Two diffractions are illustrated in Figure 4, computed from a scatter point in the Marmousi data set and displayed as a 2D matrix. The first diffraction in (a) contains a multi valued diffraction of first arrival times computed with raytracing through a smoothed version of the Marmousi velocities. The second diffraction in (b) is a wave field diffraction computed from the same location, but using wave propagation of a wavelet that includes multipathing and multiples. This figure also contains blue dots that define the location and arrival times for a family of rays emanating from the scatterpoint.

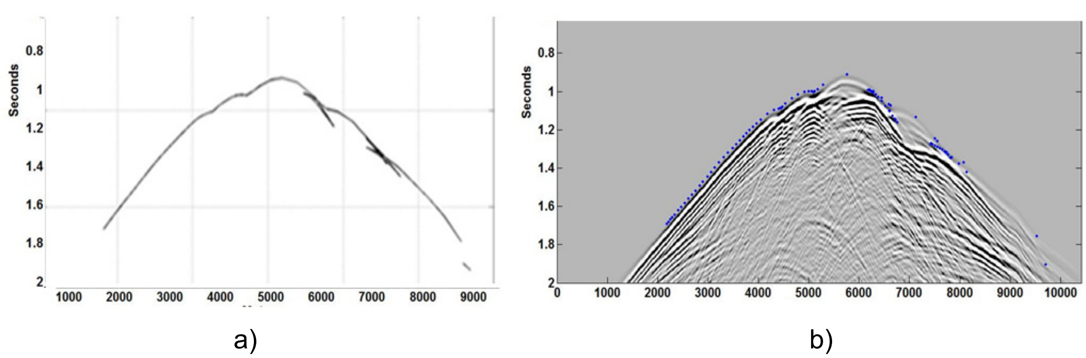

FIG. 4 Two diffractions, a) multi valued computed using raytracing, and b) full waveform using wave propagation.

A basic Kirchhoff algorithm will only use a single valued diffraction stored in vectors of traveltime and amplitudes that is much more efficient than the matrix form in Figure 4a as it contains mainly null space and is inefficient with memory usage. Use of the full wavefield in (b) is considered to be very expensive to compute, but is more reasonable for storage in a matrix form, suitable for use in Linear Algebra.

A Linear Algebra view of modelling and migration

Kirchhoff *modelling* assumes that a reflector is composed of scatterpoints, and that each scatterpoint will produce a diffraction. The sum of all diffractions creates a time section. The amplitude of the diffraction energy is defined by the amplitude of the reflectivity. This is a forward modelling process that can be represented in Linear Algebra with multidimensional arrays, **D**, **r**, and **s** that represent the diffractions, reflectivity, and seismic data respectively. A special branch of Multidimensional Linear Algebra is required to manipulate these multidimensional arrays. However, the arrays may be reduced to two dimensional (2D) arrays (matrices), or one dimensional (1D) vectors for use with conventional Linear Algebra, including Least Squares analysis (Claerbout 1998, Yousefzadeh et al. 2013, Bancroft et al. 2012). With this understanding, we use an uppercase **D** to represent a diffraction array that can be simplified to a 2D matrix, and the lower case **r** and **s** to represent data that can be simplified to 1D vectors. These definitions can apply to either time or depth migrations, to poststack or prestack migrations, and to 2D or 3D seismic data.

An advantage of using Linear Algebra is that seismic data **s** can be created with the product of the diffraction matrix with the reflectivity vector

$$\tilde{\mathbf{D}}\mathbf{r} = \mathbf{s}\,. \tag{1}$$

Kirchhoff migration is the reverse or inverse process of modelling, which sums energy along a diffraction, then places that sum at the reflector point. This summation is not a convolution process, and we are required to find a convolution type operator. In a constant velocity environment, this operator is a semi-circle. This semi-circle operator may be found by transposing two dimensions of a multidimensional diffraction array **D** to create $\mathbf{D}^{\mathbf{T}}$. Both **D** and $\mathbf{D}^{\mathbf{T}}$ are illustrated with a simple example in the appendix for modelling and migrating 2D seismic data.

We now write the migration equation as

$$\hat{\mathbf{r}} = \tilde{\mathbf{D}}^{\mathrm{T}}\mathbf{s}\,, \tag{2}$$

where $\hat{\mathbf{r}}$ is the migrated form of the reflectivity.

Seismic inversion

Rather than trying to recover the reflectivity with a transpose process, it is more desirable to obtain an estimate of the reflectivity using the inverse diffraction matrix $\mathbf{D}^{-1}$ defined as

$$\mathbf{r} = \tilde{\mathbf{D}}^{-1}\mathbf{s}, \tag{3}$$

but that is not possible as the **D** matrix is usually multi-dimensional, not square, ill-posed with evanescent energy, and unstable. We can however, multiply both sides of equation (1) with $\tilde{\mathbf{D}}^{\mathbf{T}}$

$$\tilde{\mathbf{D}}^{\mathbf{T}}\tilde{\mathbf{D}}\breve{\mathbf{r}} = \tilde{\mathbf{D}}^{\mathbf{T}}\mathbf{s}, \tag{4}$$

often referred to as the "normal equations," to get the Least Squares solution of $\breve{\mathbf{r}}$ using

$$\breve{\mathbf{r}} = \left(\tilde{\mathbf{D}}^{\mathbf{T}}\tilde{\mathbf{D}}\right)^{-1}\tilde{\mathbf{D}}^{\mathbf{T}}\mathbf{s}. \tag{5}$$

The $\tilde{\mathbf{D}}^{\mathbf{T}}\tilde{\mathbf{D}}$ matrix is referred to as the covariance matrix or resolution matrix, and requires a stabilizing factor for its inversion. These are the basic equations used for LSM and will recover a good estimate of the reflectivity $\breve{\mathbf{r}}$.

Least Squares migration using equations (4) or (5) is an expensive process and not commercially practical at this time with real seismic data. In practice, the algorithms for estimating $\breve{\mathbf{r}}$ do not invert the resolution matrix, but use an iterative solution with the conjugate gradient method.

Approximate method of inversion

The $\tilde{\mathbf{D}}^{\mathbf{T}}\tilde{\mathbf{D}}$ matrix of a Least Squares problem may be considered to be diagonally dominant, and can be approximated with the identity matrix **I**, which has the convenient inverse that equals **I**, i.e.,

$$\left(\tilde{\mathbf{D}}^{\mathbf{T}}\tilde{\mathbf{D}}\right)^{-1} \approx \left(\mathbf{I}\right)^{-1} = \mathbf{I}. \tag{6}$$

In this case, the inverted term in equation (5) is eliminated, and we get the transpose solution of equation (2). Migration is a simplification of LSM (Claerbout 1992).

In seismic applications, the $\tilde{\mathbf{D}}^{\mathbf{T}}\tilde{\mathbf{D}}$ matrix is not diagonally dominant, indicating its elimination in a conventional migration produces and inferior approximation to the inversion. The lack of diagonal dominance also makes the inversion process of LSM difficult and iterative solutions using the Jacobi or Multigrid methods are not useful. However, the Conjugate Gradient method does provide a viable solution (Yousefzadeh et al. 2010, and 2013).

The wavelet matrix

We conveniently left out any mention of a wavelet in our modelling. This is quite normal in conventional modelling and migration where we use single valued diffractions or semi-circles as it is more convenient, faster, and does a reasonable job. In these cases the wavelet is assumed to be part of the reflectivity structure. However, the wavelet should be part of the diffraction as used above with $\tilde{\mathbf{D}}$.

Let us now define a wavelet matrix $\mathbf{W}$ that can be multiplied with the single valued diffraction matrix $\bar{\mathbf{D}}$ to put wavelets on the diffractions, i.e. $\mathbf{W}\bar{\mathbf{D}} = \tilde{\mathbf{D}}$. The modelling equation becomes

$$\mathbf{W}\bar{\mathbf{D}}\mathbf{r} = \mathbf{s}, \tag{7}$$

where the reflectivity matrix $\mathbf{r}$ is a high frequency representation of the reflectivity. Recalling that $(\mathbf{W}\bar{\mathbf{D}})^{\mathbf{T}} = \bar{\mathbf{D}}^{\mathbf{T}}\mathbf{W}^{\mathbf{T}}$, the Least Squares solution is now

$$\breve{\mathbf{r}} = \left(\bar{\mathbf{D}}^{\mathrm{T}}\mathbf{W}^{\mathrm{T}}\mathbf{W}\bar{\mathbf{D}}\right)^{-1}\bar{\mathbf{D}}^{\mathrm{T}}\mathbf{W}^{\mathrm{T}}\mathbf{s}. \tag{8}$$

Removing the inversion part and going back to the migration or transpose solution we have

$$\tilde{\mathbf{r}} = \bar{\mathbf{D}}^{\mathrm{T}}\mathbf{W}^{\mathrm{T}}\mathbf{s}. \tag{9}$$

This equation implies that, when migrating with a single valued diffraction, we need to "correlate" the seismic data with the wavelet. The migration will contain a zero-phase wavelet, and have a higher signal to noise ratio (SNR), which is typical of a true Matched Filter. However, correlation of the wavelet lowers the bandwidth of the migration, so in practice, the correlation of the wavelet is not included, i.e.

$$\tilde{\mathbf{r}} \approx \bar{\mathbf{D}}^{\mathrm{T}}\mathbf{s}, \tag{10}$$

leading to the belief that migration with single valued diffractions is recovering the higher frequencies.

AN EXAMPLE OF LEAST SQUARES MIGRATION

LSM is computationally intensive and usually only simple models or small data sets are shown. Figure 4 shows a simple example of LSM with (a) a reflectivity structure, (b) a prestack migration from seismic data modelled on the structure, and (c) a corresponding LSM using the same data as (b). This simple model used four source (shot) records that produce reasonable results. Notice the wavelet remains with the migration in (b), but has been substantially removed in the LSM in (c). Both the migration in (b) and the LSM in (c) used single valued diffractions in D.

The results of the LSM may appear impressive, but the modelling process only included a small amount of random noise that enabled the high frequency content of the wavelet to reconstruct the reflectivity. There are many other benefits to LSM, such as recovering missing data, but the intent of the example in Figure 4 demonstrates that LSM does recover a higher resolution of the reflectivity than a conventional migration.

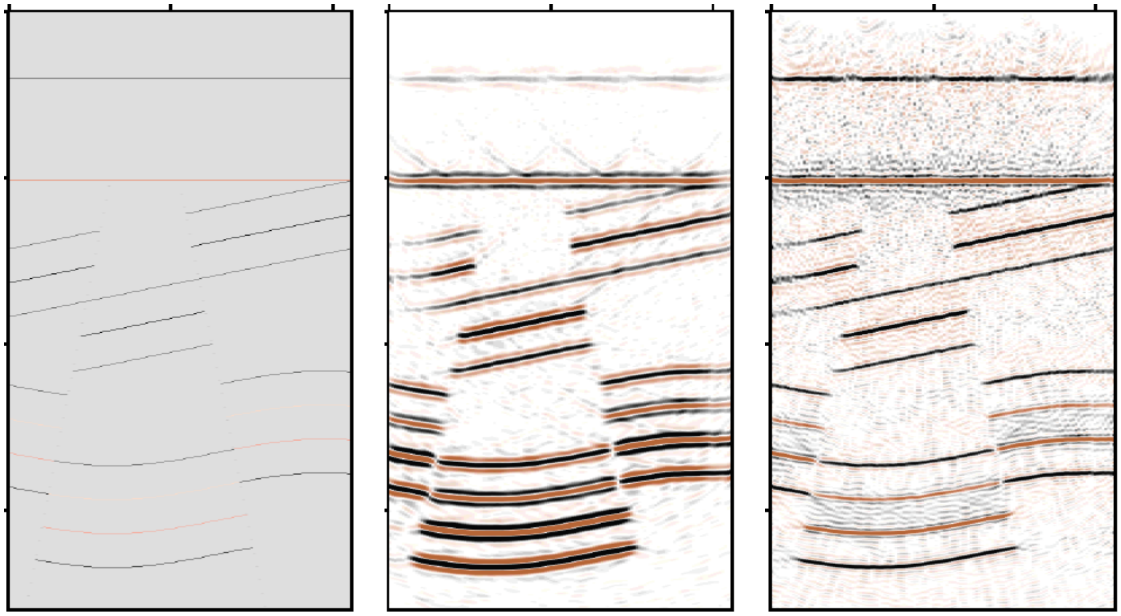

a) b) c)

FIG. 4 Illustration of a) a reflectivity structure, b) a migration, and c) a LSM.

We now use these tools to discuss the objections of DaM and present arguments for its use.

A DISCUSSIOIN OF DaM OBJECTIONS

1. Deconvolution before migration maintains the resolution of horizontal and dipping events

Figures 1 and 2 demonstrate that the resolution of the wavelet in horizontal and dipping events is restored by the migration process. A 1D temporal (trace) deconvolution before migration will therefore provide the necessary resolution enhancement for both horizontal and dipping events. This does not imply that the resolution after migration cannot be improved by DaM.

2. Deconvolution may alias the frequencies of steeply dipping migrated events

Trace deconvolution after migration increases the frequency content of a dipping event and may cause it to be aliased and harm the data. That is true to some extent when applying a trace deconvolution to steeply dipping data. However, the aliasing may not be a serious problem as the eye may be able to ignore the aliasing. If the aliasing is serious, as would be the case in sub-salt imaging, a multidimensional deconvolution that considers the dip may be required. In areas where the geological structure is less complex, such as in sedimentary basins, a trace deconvolution may be adequate.

3. Deconvolution will increase noise

The bandwidth (BW) of seismic data is considered to be that part of the amplitude spectrum where the signal to noise ratio (SNR) is greater than one. Deconvolution attempts to flatten or whiten the amplitude spectrum of both the seismic data and the noise. Identifying the new bandwidth of the data after migration may require additional signal processing or testing with a number of bandpass filters.

A quality migration should attenuate noise and increase the BW of the seismic data. Some interpreters may consider the appearance of a low noise section to be "wormy" and objectionable. Consequently, some migration algorithms add noise back to the data to "improve" its appearance. A deconvolution after migration increases the resolution of the migrated section and makes it less "wormy" and more interpretable.

Some migrations avoid the use of an appropriate antialiasing filter (AAF) to save computing time and costs, or to make a section look less wormy. In these cases, the benefit of DaM may not be realized.

4. Deconvolution will produce artifacts

Some processes overcome the time varying (non-stationary) nature of seismic data by processing parts of the data in time windows or spatial windows. These windows of data are then combined (by cut and paste) to create the total section. The edges of these windows will have abrupt changes in the wavelets, so the data are high-cut filtered to remove this discontinuity. Time varying processes may include static analysis, deconvolution, and migration.

A deconvolution applied to these cut and paste sections will enhance the discontinuities to reveal the window boundaries and be unacceptable. In this case, a deconvolution after migration may be more desirable for a client to show imperfection in the algorithm.

5. Kirchhoff migration already uses whitening operators

A Kirchhoff migration that uses a single valued function for the diffraction is much faster and requires less memory. It does <u>not</u> convolve with the extra wavelet as required by a true matched filter, but does produce a migrated wavelet with a higher resolution. This process has been considered to be a form of spectral whitening, and that any additional spectral whitening is not required.

Consider again the Least Squares equation (8) and rewrite it in a form for some kind of dimensional analysis $\langle \breve{\mathbf{r}} \rangle$ that includes a wavelet with the seismic data, i.e.,

$$\langle \breve{\mathbf{r}} \rangle \sim> \frac{\bar{D}^T W^T s}{\bar{D}^T W^T W \bar{D}} = \frac{s}{W\bar{D}} . \tag{11}$$

When simplifying the inversion to a transpose process on the right of equation (11), we replace $1/D$ with D^T or

$$\frac{s}{W\bar{D}} \approx \frac{\bar{D}^T s}{W} , \tag{12}$$

where the conventional migration $\tilde{\mathbf{r}} = \bar{\mathbf{D}}^{\mathbf{T}} \mathbf{s}$ using a single valued diffraction (equation (10)) still requires the removal of another wavelet to match $\breve{\mathbf{r}}$ of equation (11). The prestack migration example in Figure 4b did use single valued diffractions in **D**, and the wavelet from modelling is still present in the data.

REASONS WHY DECONVOLVOLUTON IS NECESSARY AFTER MIGRATION

The used of DaM is dictated by the inversion process

Conventional migration that uses the transpose process assumes that the "resolution matrix" $\left(\tilde{\mathbf{D}}^{\mathrm{T}}\tilde{\mathbf{D}}\right)^{-1}$ is not part of the process. However, it is this part of the inversion process that increases the resolution of the data. Even the use of a single valued diffraction does not produce the same result as the LSM. The inversion can be simulated with a trace deconvolution that tends to flatten (or whiten) the amplitude spectrum of the trace. In areas with complex geology, a more sophisticated multidimensional deconvolution process could be used that involves the dips of the reflectors.

The example of LSM in Figure 4 indicates that the resolution of the prestack migration in (b) could be increased by a deconvolution process. Since the structure of this example is relatively horizontal, we contend that a simple spiking deconvolution would produce a result similar to the LSM in (c).

The imaging condition

A common method of estimating the reflectivity R was presented by Claerbout in 1971 in which he defined the down-going energy D just above a reflector, and the up-going reflected energy U just above a reflector, all defined in the frequency domain. The reflectivity was defined by

$$R = \frac{U}{D} \cdot \tag{13}$$

Instabilities in this computation lead to a simplification that replaced the inversion with D by the product of the conjugate, D^*,

$$R \approx UD^* \cdot \tag{14}$$

In the time domain, this becomes a cross-correlation of the seismic data that is migrated to the depth of a reflector U, with modelled seismic data at a depth just above the reflector D. Notice that the inversion of equation (13) is replaced by the correlation of equation (14), similar to the transpose process of a conventional migration. This correlation process does not recover the bandwidth of the reflectivity that could be achieved with a process similar to equation (13). A deconvolution after migration will tend to recover the bandwidth lost in the correlation process.

A heuristic argument for deconvolution after migration

Deconvolution essentially tries to flatten the amplitude spectrum of the seismic data. However, when we flatten the spectrum we flatten both the signal and the noise. We generally consider the bandwidth of the signal, or reflection energy, to be the area of the amplitude spectrum where the signal is greater than the noise, i.e., when the signal to noise ratio (SNR) is greater than one, i.e., SNR > 1. This is illustrated in Figure 5, which contains an exaggerated cartoon sketch of the amplitude spectrum of seismic data and three levels of noise. The first noise level represents the noise level in the raw data, the second is the reduced noise after stacking, and the third is the noise level after migration. Each time we reduce noise we increase the frequency band where the SNR is greater than one, i.e., from F_r to F_s and then to F_m. Deconvolution tends to flatten the amplitude spectrum in each of these bands where a broader bandwidth corresponds to an increase in resolution. Bandpass filters are designed to attenuate the energy when the SNR < 1.

Figure 5 illustrates the improved bandwidth at the higher frequencies when the noise is reduced. Similar improvements are also obtained with DaM at the lower frequencies. This may be especially important to other inversion processes such as model based inversions (Lindseth 1979, Russell et al. 1991, Hampson, et al. 2005) and full waveform inversion (FWI) in which migration is part of the inversion process.

Poststack migration benefits from the stacking process, and it is common practice to apply a deconvolution at this stage of the processing. Improved resolution can still be obtained with DaM.

Prestack migration does not stack the data before the migration, thus does not benefit from the improved resolution of deconvolution after stacking. It tends to have spectral whitening over a bandwidth equivalent that of the "Raw noise" in Figure 5. However, a prestack migration does have an improved SNR due to the migration and stacking, and have a greater bandwidth where SNR > 1. It will benefit greatly from a deconvolution to whiten the spectrum over this increased bandwidth. Consequently, the bandwidth gained through deconvolution after prestack migration is considerably greater than that for poststack migration, and DaM should be considered essential in this case.

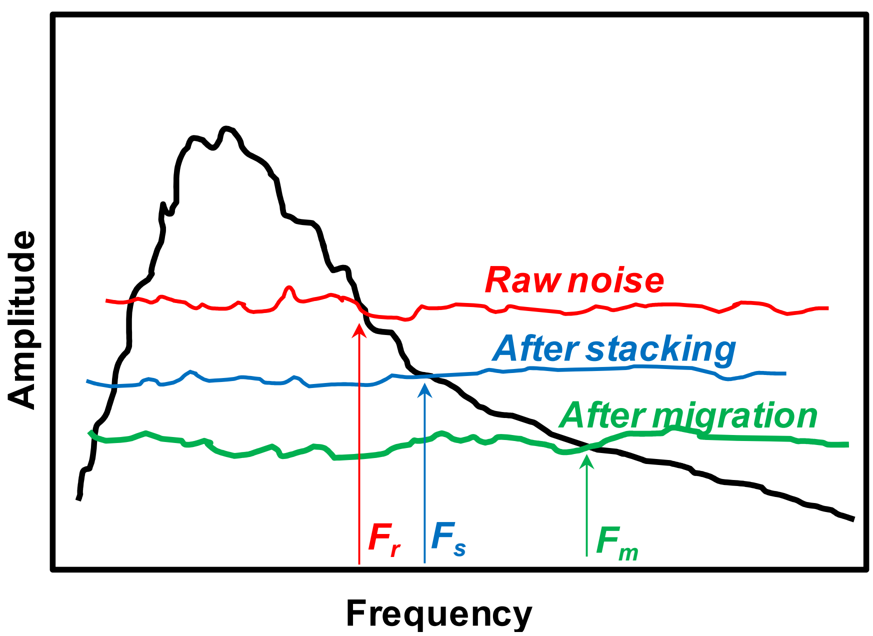

FIG. 5 Cartoon illustrating the increased bandwidth of the SNR as the noise level is reduced after stacking and then after migration.

EXAMPLES OF DECONVOLUTION AFTER MIGRATION

NE British Columbia data

A noisy 2D seismic line was chosen from a project in NE British Columbia, Canada, which used a low-dwell sweep from 1 to 100 Hz, into the vertical component of a 3C phone. The data were processed to a flat datum at the central elevation. Deconvolution, gain recovery, and statics were applied to the prestack data. The data were then prestack time migrated using the Equivalent Offset method (EOM). The migrated section is shown in Figure 6a, and the migration followed by a spiking deconvolution is shown in Figure 6b. The increase in resolution with deconvolution after migration is evident.

The amplitude spectra of the data are compared in Figure 7, with (a) the prestack migration, and (b) the same data with a spiking deconvolution applied after the migration. Note the flatter amplitudes of the deconvolved section in the seismic band, and the broader pass band at the lower and higher frequencies.

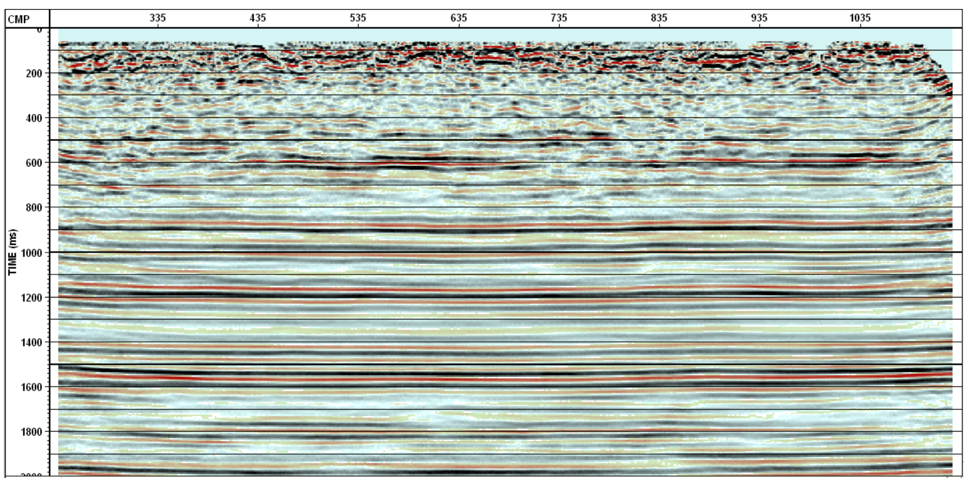

a)

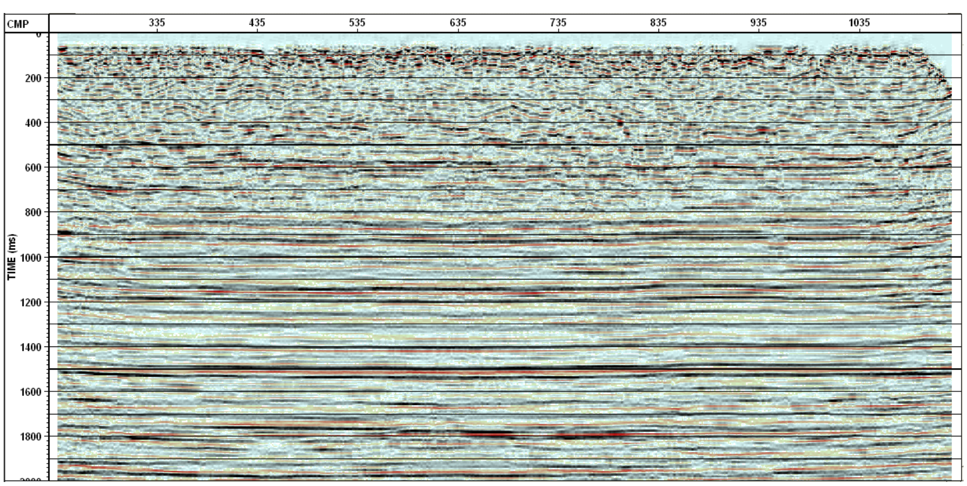

b)

FIG. 6 Seismic sections: a) a prestack migrated section and b) deconvolution applied to the section in (a).

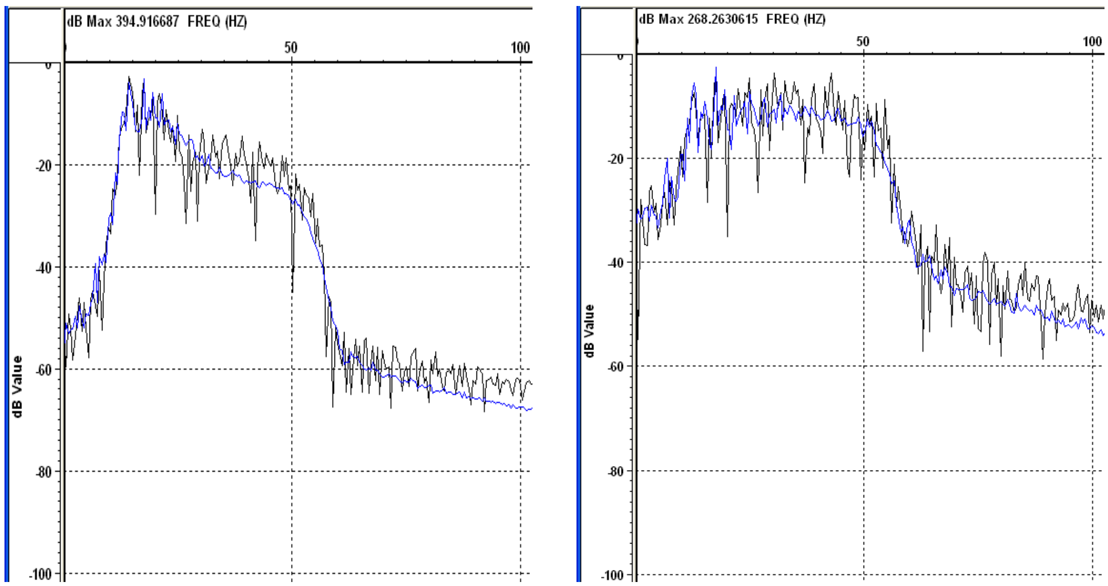

a) b)

FIG. 7 Amplitude spectra of a) the prestack migrated data, and b) the migrated data with deconvolution.

South America data

The following data are from a 3D project somewhere in South America. The data were processed commercially and completed with a high quality prestack time migration. It was difficult to convince the persons processing the data to apply a deconvolution after the migration. The results are shown in the following sections of Figure 8. Zoom displays are included in Figure 9 that focuse on an area of significant improvement in resolution when using DaM.

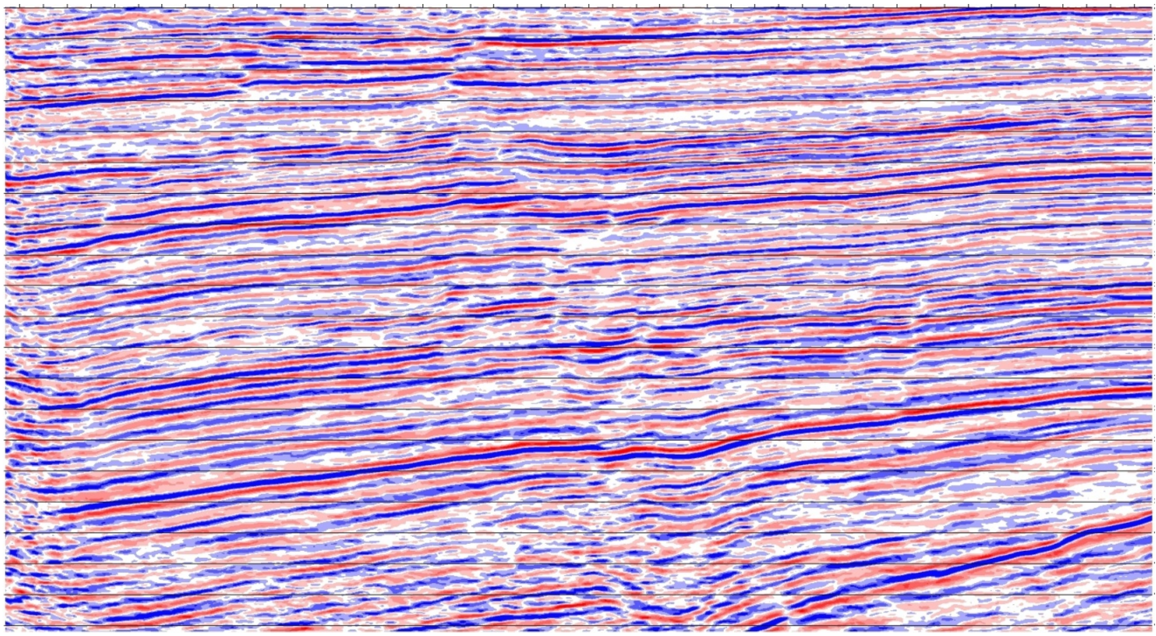

a)

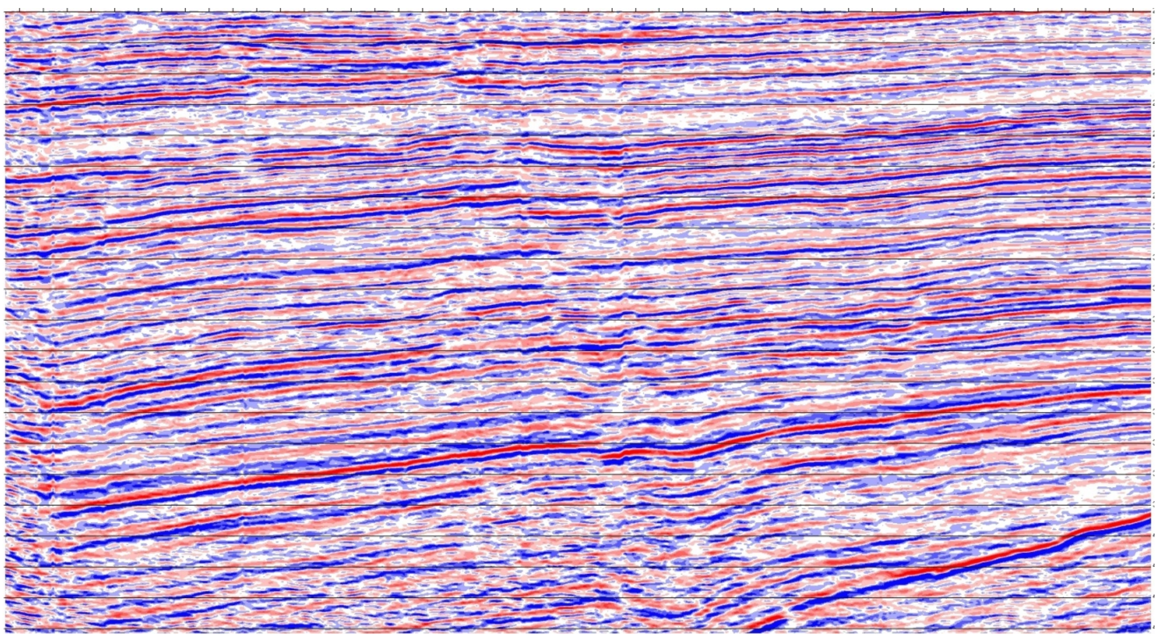

b)

FIG. 8 a) Prestack migration followed in b) with a spiking deconvolution applied to (a).

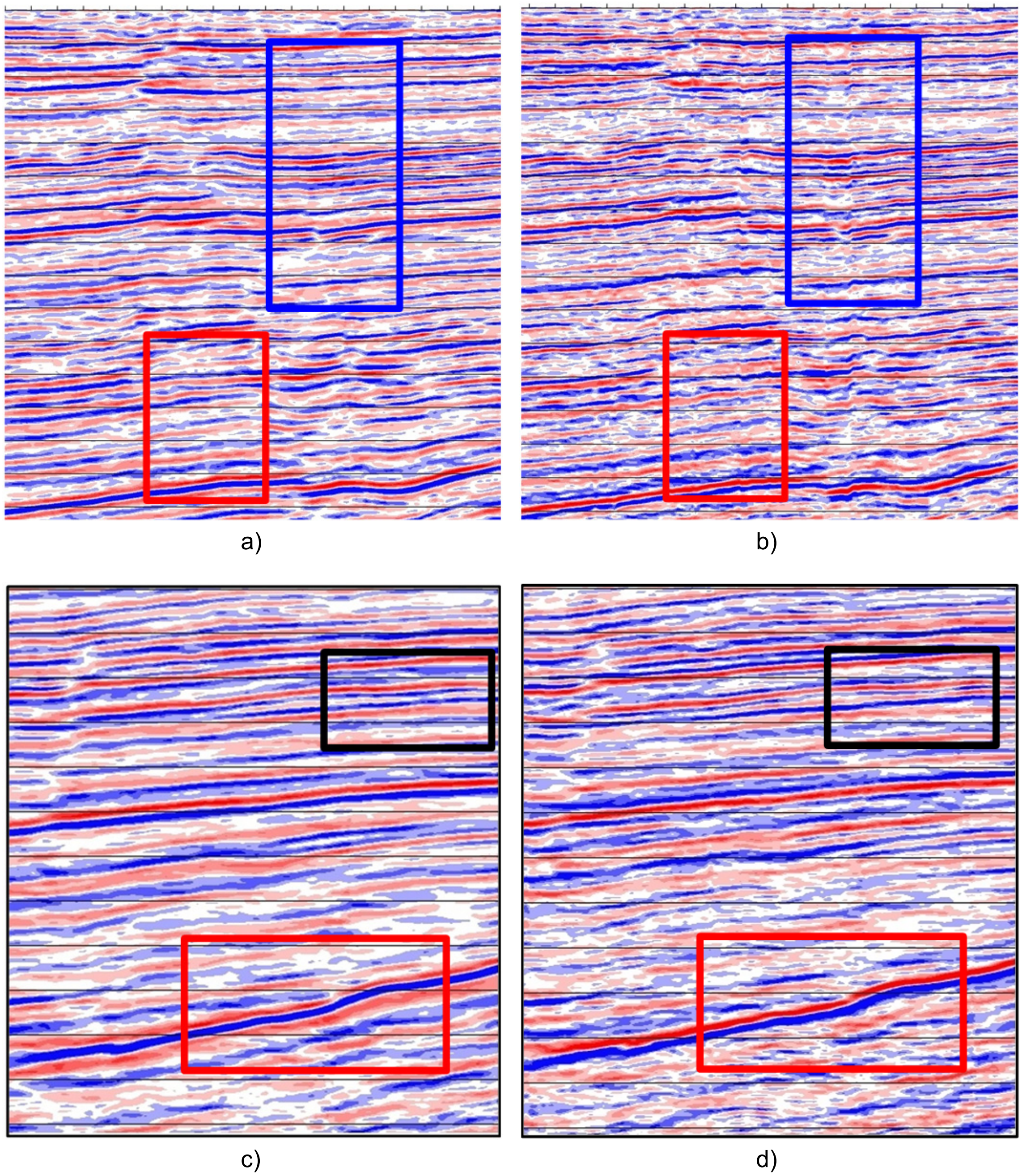

FIG. 9 Zoom of the data with a) showing one portion and b) its equivalent deconvolution. Part c) and d) show a similar comparison for another part of the data.

COMMENTS AND CONCLUSIONS

Least Squares migration performs an inversion of seismic data that is independent of dip, implying that it recovers the optimum resolution for horizontal and dipping events. We have only approximated this process with a trace deconvolution that is appropriate for data with shallow dips. A more elaborate multidimensional deconvolution that considers dip may be more appropriate in structured environments.

A simple spiking deconvolution was applied in the examples. A non-stationary or time varying deconvolution such as Gabor deconvolution (Margrave et al, 2011) should produce greater improvements over a larger time portion of the data.

A clean, noise reduced migration may appear wormy to an interpreter, and noise may be deliberately added to improve its appearance. A deconvolution after the migration will make the section appear less wormy, with the added benefit of increased resolution.

Deconvolution should be applied after a quality migration.

Deconvolution after migration is even more important after a prestack migration.

ACKNOWLEDGEMENTS

We thank the oil company and the contactor for giving me permission to show the data.

We wish to thank the CREWES sponsors for their continued support.

REFERENCES

Bancroft, J. C., T. Guirigay, and H. Isaac, 2012, Deconvolution after migration, CSEG Recorder.

Claerbout, J. F., 1971, Toward a unified theory of reflector mapping, Geophysics, Vol. 36, No. 3, 467-481.

Claerbout, J. F., 1992, Earth Sounding Analysis: Processing versus Inversion, Blackwell

Claerbout, J. F., 1998, Multidimensional recursive filters via a helix, Presented at the SEG research workshop, Vail, CO, see also http://sepwww.stanford.edu/data/media/public/abstracts/seg98/jon.pdf

Lindseth, R. O., 1979, Synthetic sonic logs - A process for stratigraphic interpretation: Geophysics, Vol. 44 , No.1, 3-26.

Margrave, G. F., M.P Lamoureux, and D.C. Henley, 2011, Gabor deconvolution: Estimating reflectivity by nonstationary deconvolution of seismic data, Geophysics, Vol. 76, No. 2

Russell, B., and D. Hampson, 1991, Comparison of poststack inversion method: 61st Ann. Mtg., Soc. Expl. Geophys., Expanded Abstracts, 876-878.

Hampson, D., Russell, B., and Bankhead, B., 2005, Simultaneous inversion of pre-stack seismic data: Ann. Mtg. Abstracts, Society of Exploration Geophysicists.

Yousefzadeh, A., and Bancroft, J. C., 2010, Solving least squares Kirchhoff migration using multigrid methods: 80th Annual International Meeting, Society of Exploration Geophysicists, Expanded Abstract, 3135-3139.

Yousefzadeh 2013, High Resolution Seismic Imaging using Least Squares Migration, PhD Dissertation, Department of Geoscience, University of Calgary.

APPENDIX

A 4D diffraction matrix **G** for 2D seismic data is shown below in Figure A1. It shows a 2D array of reflectivity [***k***, ***l***] that contains 2D sub-arrays of diffractions [***i***, ***j***]. Each diffraction has 4 rows of time (***i*** = 1 to I) and 5 columns or traces (***j*** = 1 to J). The reflectivity structure has 3 depth samples (***k*** = 1 to K) in 5 columns or spatial locations, (***l*** = 1 to L). The 2D transpose of **G** is formed by transposing the ***i*** and ***k*** elements,

$$\left[\mathbf{G}(i,j,k,l)\right]^{\mathrm{T}} = \mathbf{G}(k,j,i,l), \tag{15}$$

as shown in Figure A2 that displays the migration operators as approximate semicircles in each black […], that become sub-matrices of the migration matrix […].

$$\begin{array}{cc}
 & \qquad j \qquad\qquad\qquad\qquad\qquad\qquad l \\
\begin{array}{c} i \\ \\ \\ k \end{array} &
\left[\begin{array}{ccccc}
\begin{bmatrix}1&.&.&.&.\\.&1&.&.&.\\.&.&1&.&.\\.&.&.&1&.\end{bmatrix} &
\begin{bmatrix}.&1&.&.&.\\1&.&1&.&.\\.&.&.&1&.\\.&.&.&.&1\end{bmatrix} &
\begin{bmatrix}.&.&1&.&.\\.&1&.&1&.\\1&.&.&.&1\\.&.&.&.&.\end{bmatrix} &
\begin{bmatrix}.&.&.&1&.\\.&.&1&.&1\\.&1&.&.&.\\1&.&.&.&.\end{bmatrix} &
\begin{bmatrix}.&.&.&.&1\\.&.&.&1&.\\.&.&1&.&.\\.&1&.&.&.\end{bmatrix} \\
\begin{bmatrix}.&.&.&.&.\\1&1&.&.&.\\.&.&1&.&.\\.&.&.&1&.\end{bmatrix} &
\begin{bmatrix}.&.&.&.&.\\1&1&1&.&.\\.&.&.&1&.\\.&.&.&.&1\end{bmatrix} &
\begin{bmatrix}.&.&.&.&.\\.&1&1&1&.\\1&.&.&.&1\\.&.&.&.&.\end{bmatrix} &
\begin{bmatrix}.&.&.&.&.\\.&.&1&1&1\\.&1&.&.&.\\1&.&.&.&.\end{bmatrix} &
\begin{bmatrix}.&.&.&.&.\\.&.&.&1&1\\.&.&1&.&.\\.&1&.&.&.\end{bmatrix} \\
\begin{bmatrix}.&.&.&.&.\\.&.&.&.&.\\1&1&1&.&.\\.&.&.&1&.\end{bmatrix} &
\begin{bmatrix}.&.&.&.&.\\.&.&.&.&.\\1&1&1&1&.\\.&.&.&.&1\end{bmatrix} &
\begin{bmatrix}.&.&.&.&.\\.&.&.&.&.\\1&1&1&1&1\\.&.&.&.&.\end{bmatrix} &
\begin{bmatrix}.&.&.&.&.\\.&.&.&.&.\\.&1&1&1&1\\1&.&.&.&.\end{bmatrix} &
\begin{bmatrix}.&.&.&.&.\\.&.&.&.&.\\.&.&1&1&1\\.&1&.&.&.\end{bmatrix}
\end{array}\right]
\end{array}$$

FIG. A1 The 4D diffraction matrix

$$\begin{array}{cc}
 & \qquad j \qquad\qquad\qquad\qquad\qquad\qquad l \\
\begin{array}{c} k \\ \\ \\ i \end{array} &
\left[\begin{array}{ccccc}
\begin{bmatrix}1&.&.&.&.\\.&.&.&.&.\\.&.&.&.&.\end{bmatrix} &
\begin{bmatrix}.&1&.&.&.\\.&.&.&.&.\\.&.&.&.&.\end{bmatrix} &
\begin{bmatrix}.&.&1&.&.\\.&.&.&.&.\\.&.&.&.&.\end{bmatrix} &
\begin{bmatrix}.&.&.&1&.\\.&.&.&.&.\\.&.&.&.&.\end{bmatrix} &
\begin{bmatrix}.&.&.&.&1\\.&.&.&.&.\\.&.&.&.&.\end{bmatrix} \\
\begin{bmatrix}.&1&.&.&.\\1&1&.&.&.\\.&.&.&.&.\end{bmatrix} &
\begin{bmatrix}1&.&1&.&.\\1&1&1&.&.\\.&.&.&.&.\end{bmatrix} &
\begin{bmatrix}.&1&.&1&.\\.&1&1&1&.\\.&.&.&.&.\end{bmatrix} &
\begin{bmatrix}.&.&1&.&1\\.&.&1&1&1\\.&.&.&.&.\end{bmatrix} &
\begin{bmatrix}.&.&.&1&.\\.&.&.&1&1\\.&.&.&.&.\end{bmatrix} \\
\begin{bmatrix}.&.&1&.&.\\.&.&1&.&.\\1&1&1&.&.\end{bmatrix} &
\begin{bmatrix}.&.&.&1&.\\.&.&.&1&.\\1&1&1&1&.\end{bmatrix} &
\begin{bmatrix}1&.&.&.&1\\1&.&.&.&1\\1&1&1&1&1\end{bmatrix} &
\begin{bmatrix}.&1&.&.&.\\.&1&.&.&.\\.&1&1&1&1\end{bmatrix} &
\begin{bmatrix}.&.&1&.&.\\.&.&1&.&.\\.&.&1&1&1\end{bmatrix} \\
\begin{bmatrix}.&.&.&1&.\\.&.&.&1&.\\.&.&.&1&.\end{bmatrix} &
\begin{bmatrix}.&.&.&.&1\\.&.&.&.&1\\.&.&.&.&1\end{bmatrix} &
\begin{bmatrix}.&.&.&.&.\\.&.&.&.&.\\.&.&.&.&.\end{bmatrix} &
\begin{bmatrix}1&.&.&.&.\\1&.&.&.&.\\1&.&.&.&.\end{bmatrix} &
\begin{bmatrix}.&1&.&.&.\\.&1&.&.&.\\.&1&.&.&.\end{bmatrix}
\end{array}\right]
\end{array}$$

FIG. A2 The 4D transpose of the diffraction matrix.

Figure A3 shows a 3D diffraction array and its transpose for one vertical array of scatterpoints at a fixed spatial location (x). The medium has constant velocities, so the diffractions have a hyperbolic shape and the migration operators are semicircular. Figure A3a shows the diffraction array for modelling with three green diffractions in (x, t) at three different depths (z). These three, and all possible diffractions, form the shape of a cone. It represents the central location of the column sub-matrices in Figures A1. A horizontal slice through the cone is represented by the red semicircle.

Figure A3b shows the 2D transpose of the diffraction array that rotates the vertical cone in (a) to the horizontal cone in (b). Now, the red vertical intersection in (x, z) at a specific time (t) is the semicircle that represents the migration operator.

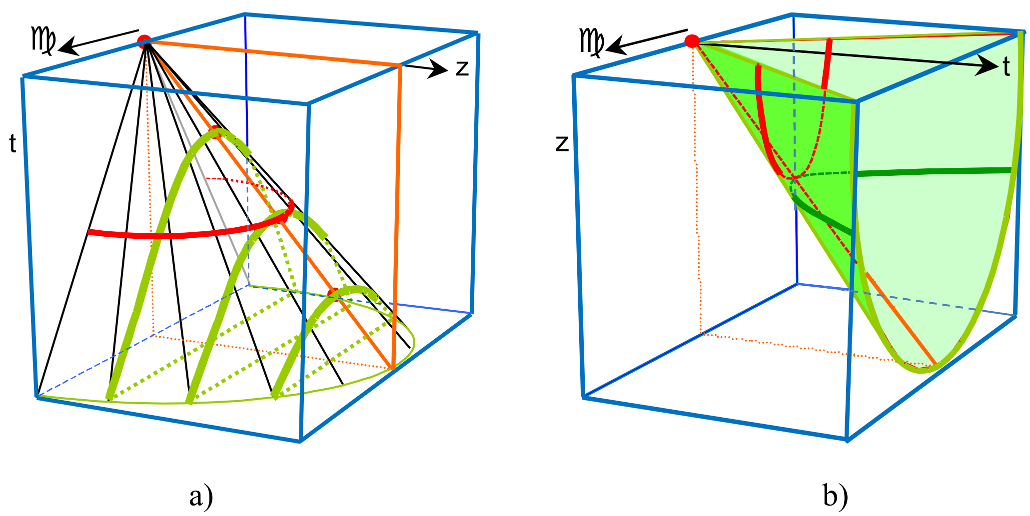

FIG. A3 A 3D view of a 3D diffraction array **G** for a) modelling and a) the transpose $\mathbf{G}^T$ for migration.

If the velocity varied, the diffractions become non-hyperbolic and the diffraction surface will deviate from the cone, and could become multivalued with caustics. In that case, for 2D seismic data, a different 3D diffraction array is required for each spatial location in x, creating the 4D diffraction array as indicated in Figure A1.

Additional complexity could be added to the diffraction array by using diffractions computed using wave propagation. In that case, the inside of the "cone" with contain caustics, multiples, and wavelets. It is these situations where practical use of the arrays may become viable.